TROSY-type Triple-Resonance Experiments for Sequential NMR Assignments of Large Proteins

Michael Salzmann,[†,‡] Gerhard Wider,[†] Konstantin Pervushin,[†] Hans Senn,[‡] and Kurt Wüthrich*[,†]

Contribution from the Institut für Molekularbiologie und Biophysik, Eidgenössische Technische Hochschule Hönggerberg, CH-8093 Zürich, Switzerland

Received September 25, 1998. Revised Manuscript Received November 24, 1998

Abstract: Transverse relaxation-optimized spectroscopy (TROSY) was implemented in the four triple resonance experiments [^{15}N,^{1}H]-TROSY-HN(CO)CA, [^{15}N,^{1}H]-TROSY-HN(CA)CO, [^{15}N,^{1}H]-TROSY-HNCACB, and [^{15}N,^{1}H]-TROSY-HN(CO)CACB. Combined with [^{15}N,^{1}H]-TROSY-HNCA and [^{15}N,^{1}H]-TROSY-HNCO (Salzmann, M.; Pervushin, K.; Wider, G.; Senn, H. Wüthrich, K. *Proc. Natl. Acad. Sci. U.S.A.* **1998**, 13585−13590) these experiments represent a suite of TROSY-type triple resonance experiments that enables sequential backbone assignment of proteins. When used with the 23 kDa ^{2}H/^{13}C/^{15}N-labeled protein gyrase 23B, a comparison with the corresponding conventional NMR experiments showed, on average over the entire amino acid sequence, a 3-fold sensitivity gain for each of the four experiments. The use of the TROSY principle in triple resonance experiments thus promises to enable resonance assignments for significantly larger proteins than what is achievable today with the corresponding conventional NMR experiments.

Introduction

The assignment of chemical shifts to the individual nuclei is a prerequisite of protein structure determination by nuclear magnetic resonance (NMR[1]) spectroscopy.[2,3] Assignments for the largest proteins so far have been obtained by using triple resonance experiments with ^{13}C/^{15}N-labeled proteins, which use through-bond scalar coupling connectivities for sequential assignment of the backbone $^{1}H^{N}$, ^{15}N, $^{13}C^{\alpha}$, and ^{13}CO spins.[4−8] Size limitations for the use of triple-resonance experiments arise from fast transverse relaxation of the heteronuclei, especially $^{13}C^{\alpha}$, which is efficiently relaxed by dipole−dipole (DD) interactions with $^{1}H^{\alpha}$. Deuteration significantly decreases the transverse $^{13}C^{\alpha}$ relaxation rate and extends the accessible molecular size range,[9] but transverse ^{15}N relaxation during coherence transfer steps is only little affected by deuteration.[10] In contrast, transverse relaxation-optimized spectroscopy (TROSY)[11−13] yields substantial reduction of the transverse relaxation rates in $^{15}N-^{1}H^{N}$ moieties by constructive use of the interference between DD coupling and chemical shift anisotropy (CSA) interactions. Previously, the implementation of [^{15}N,^{1}H]-TROSY in the HNCA and HNCO experiments[10] yielded more than 3-fold sensitivity improvement when applied to ^{2}H/^{13}C/^{15}N-labeled proteins, and a significant gain in sensitivity was also obtained for protonated proteins. In this paper we describe the implementation of [^{15}N,^{1}H]-TROSY in additional triple-resonance NMR experiments that are commonly used for the sequential assignment of ^{2}H/^{13}C/^{15}N-labeled proteins, i.e., [^{15}N,^{1}H]-TROSY-HN(CO)CA, [^{15}N,^{1}H]-TROSY-HN(CA)CO, [^{15}N,^{1}H]-TROSY-HNCACB, and [^{15}N,^{1}H]-TROSY-HN(CO)CACB.

Experimental Section

All spectra were recorded at 20 °C with the same 1 mM sample of uniformly ^{2}H/^{13}C/^{15}N-labeled gyrase 23B[14,15] in a mixed solvent of 95% H_2O/5% D_2O at pH 6.5, using a Bruker DRX-750 spectrometer equipped with four radio frequency (rf) channels for generating the ^{1}H, ^{2}H, ^{13}C, and ^{15}N rf pulses, a pulsed field gradient unit, and a triple-resonance probehead with an actively shielded *z*-gradient coil. The following parameter settings were used for the individual experi-

* Address correspondence to this author.
† Eidgenössische Technische Hochschule Hönggerberg.
‡ F. Hoffmann-La Roche AG, Pharma Research, CH-4070 Basel, Switzerland.

(1) Abbreviations: CSA, chemical shift anisotropy; COSY, correlation spectroscopy; ct, constant time; DD, dipole−dipole; INEPT, insensitive nuclei enhanced by polarization transfer; NMR, nuclear magnetic resonance; PFG, pulsed field gradient; rf, radio frequency; ST2-PT, single transition-to-single transition polarization transfer; TPPI, time-proportional phase incrementation; TROSY, transverse relaxation-optimized spectroscopy; 3D, three-dimensional.

(2) Wüthrich, K.; Wider, G.; Wagner, G.; Braun, W. *J. Mol. Biol.* **1982**, *155*, 311−319.
(3) Wüthrich, K. *NMR of Proteins and Nucleic Acids*; Wiley: New York, 1986.
(4) Montelione, G. T.; Wagner, G. *J. Am. Chem. Soc.* **1989**, *111*, 1, 5474−5475. Ikura, M.; Kay, L. E.; Bax, A. *Biochemistry* **1990**, *29*, 4659−4667. Bax, A.; Grzesiek, S. *Acc. Chem. Res.* **1993**, *26*, 131−138. Edison, A. S.; Abildgaard, F.; Westler, W. M.; Mooberry, E. S.; Markley, J. *Methods Enzymol.* **1994**, *239*, 3−79.
(5) Yamazaki, T.; Lee, W.; Revington, M.; Matiello, D. L.; Dahlquist, F. W.; Arrowsmith, C. H.; Kay, L. E. *J. Am. Chem. Soc.* **1994**, *116*, 6464−6465.
(6) Yamazaki, T.; Lee, W.; Arrowsmith, C. H.; Muhandiram, D. R.; Kay, L. E. *J. Am. Chem. Soc.* **1994**, *116*, 11655−11666.
(7) Shan, X.; Gardner, K. H.; Muhandiram, D. R.; Rao, N. S.; Arrowsmith, C. H.; Kay, L. E. *J. Am. Chem. Soc.* **1996**, *118*, 6570−6579.
(8) Wider, G. *Prog. NMR Spectrosc.* **1998**, *32*, 193−275.
(9) LeMaster, D. M. *Prog. NMR Spectrosc.* **1994**, *26*, 371−419. Kay, L. E.; Gardner, K. H. *Curr. Op. Struct. Biol.* **1997**, *7*, 722−731.
(10) Salzmann, M.; Pervushin, K.; Wider, G.; Senn, H.; Wüthrich, K. *Proc. Natl. Acad. Sci. U.S.A.* **1998**, *95*, 13585−13590.
(11) Pervushin, K.; Riek, R.; Wider, G.; Wüthrich, K. *Proc. Natl. Acad. Sci. U.S.A.* **1997**, *94*, 12366−12371.
(12) Pervushin, K.; Wider, G.; Wüthrich, K. *J. Biomol. NMR* **1998**, *12*, 345−348.
(13) Pervushin, K.; Riek, R.; Wider, G.; Wüthrich, K. *J. Am. Chem. Soc.* **1998**, *120*, 6394−6400.
(14) Lewis, R. J.; Singh, O. M.; Smith, C. V.; Skarzynski, T.; Maxwell, A.; Wonacott, A. J.; Wigley, D. B. *EMBO J.* **1996**, *15*, 1412−1420.
(15) Wigley, D. B. *Annu. Rev. Biophys. Biomol. Struct.* **1995**, *24*, 185−208. Maxwell, A. *Trends Microbiol.* **1997**, *5*, 102−109.

10.1021/ja9834226 CCC: $18.00
Published on Web 02/03/1999

ments: *[^{15}N,^{1}H]-TROSY-HN(CO)CA*: data size 26(t_1) × 24(t_2) × 512(t_3) complex points; t_{1max}(^{15}N) = 10.8, t_{2max}(^{13}C$^{\alpha}$) = 4.8, and t_{3max}(^{1}H) = 48.7 ms; spectral widths in ω_1(^{15}N), ω_2(^{13}C$^{\alpha}$), and ω_3(^{1}H) 2400, 5000, and 10504 Hz, respectively; 32 scans per increment were acquired and the data set was zero-filled to 64(t_1) × 64(t_2) × 1024(t_3) complex points. *[^{15}N,^{1}H]-TROSY-HN(CA)CO*: 26(t_1) × 30(t_2) × 512(t_3) complex points; t_{1max}(^{15}N) = 10.8, t_{2max}(^{13}CO) = 12.0, and t_{3max}(^{1}H) = 48.7 ms; spectral widths in ω_1(^{15}N), ω_2(^{13}CO), and ω_3(^{1}H) 2400, 2500, and 10504 Hz, respectively; 24 scans per increment were acquired and the data set was zero-filled to 64(t_1) × 64(t_2) × 1024(t_3) complex points. *[^{15}N,^{1}H]-TROSY-HNCACB*: 26(t_1) × 42(t_2) × 512(t_3) complex points; t_{1max}(^{15}N) = 10.8, t_{2max}(^{13}C$^{\alpha/\beta}$) = 4.4, and t_{3max}(^{1}H) = 48.7 ms; spectral widths in ω_1(^{15}N), ω_2(^{13}C$^{\alpha/\beta}$), and ω_3(^{1}H) 2400, 9615, and 10504 Hz, respectively; 32 scans per increment were acquired and the data set was zero-filled to 64(t_1) × 128(t_2) × 1024(t_3) complex points. *[^{15}N,^{1}H]-TROSY-HN(CO)CACB*: 26(t_1) × 33(t_2) × 512(t_3) complex points; t_{1max}(^{15}N) = 10.8, t_{2max}(^{13}C$^{\alpha/\beta}$) = 3.4, and t_{3max}(^{1}H) = 48.7 ms; spectral widths in ω_1(^{15}N), ω_2(^{13}C$^{\alpha/\beta}$), and ω_3(^{1}H) 2400, 9615, and 10504 Hz, respectively; 32 scans per increment were acquired and the data set was zero-filled to 64(t_1) × 128(t_2) × 1024(t_3) complex points. Identical experimental settings were used with the corresponding conventional triple-resonance experiments. Prior to Fourier transformation the data matrices were multiplied with a 75°-shifted sine bell window in the indirect dimensions and a 60°-shifted sine bell window in the acquisition dimension.[16] Data processing was performed with the program PROSA,[17] and for the data analysis the program XEASY[18] was used.

Methods

For the incorporation of TROSY into the triple-resonance experiments discussed in this paper, we followed the procedure developed recently for the HNCA and HNCO experiments,[10] yielding [^{15}N,^{1}H]-TROSY-HN(CO)CA, [^{15}N,^{1}H]-TROSY-HN(CA)CO, [^{15}N,^{1}H]-TROSY-HNCACB, and [^{15}N,^{1}H]-TROSY-HN(CO)CACB (Figure 1 a−d). The four experiments differ only in the pulses and delays applied between the time points *c* and *k*. The common features include that both the ^{1}H and ^{15}N steady-state magnetizations are used at the outset of the experiment[12,13] and that there is a ^{1}H−^{15}N INEPT transfer between time points *a* and *c*. At time points *a*, *b*, and *k*, the water magnetization is flipped back to the +*z*-axis by using selective pulses on the water resonance.[19] From time point *k* onward the ST2-PT element transfers the ^{15}N single transition to the ^{1}H single transition selected in TROSY.[12,13] TROSY is active on ^{15}N during the first ^{15}N−^{13}C INEPT between time points *c* and *d*, and during the reverse ^{13}C−^{15}N INEPT between *i* and *k*, which encompasses the constant time (ct) ^{15}N evolution period, and on ^{1}H^{N} during data acquisition.

The individual experimental schemes of Figure 1a−d are closely related to the corresponding conventional triple-resonance NMR experiments, which have been discussed in the literature in detail.[4] Therefore, we give only a brief outline of the coherence flow in each experiment. In the [^{15}N,^{1}H]-TROSY-HN(CO)CA experiment (Figure 1a) we have

$$H_i \rightarrow \underline{N_i \rightarrow CO_{i-1}} \rightarrow C^{\alpha}_{i-1}(t_2) \rightarrow \underline{CO_{i-1} \rightarrow N_i(t_1)} \rightarrow \underline{H_i(t_3)} \quad (1)$$

where *H*, *N*, C^{α}, and *CO* represent the ^{1}H^{N}, ^{15}N, ^{13}C$^{\alpha}$, and ^{13}CO magnetizations, t_1 and t_2 are the ^{15}N and ^{13}C evolution times, t_3 is the ^{1}H acquisition time, and the indices *i* and *i−1* indicate two neighboring residues in the amino acid sequence. The time periods where TROSY is active are underlined, *i.e.* the ^{15}N−^{13}CO INEPT, the reverse INEPT and the ct ^{15}N evolution period t_1, and the data acquisition period, t_3. After the ^{1}H−^{15}N INEPT the magnetization is transferred from ^{15}N via ^{13}CO to ^{13}C$^{\alpha}$ between time points *c* and *e*. Between *f* and *g*, the ^{13}C$^{\alpha}$ magnetization evolves due to the ^{13}C$^{\alpha}$ chemical shift, since ^{13}CO is decoupled and the maximal evolution time, t_{2max}, is usually chosen short to minimize the influence of the scalar couplings between ^{13}C$^{\alpha}$ and ^{13}C$^{\beta}$, and between ^{13}C$^{\alpha}$ and ^{15}N, respectively. Between the time points *h* and *i* the magnetization is transferred back from ^{13}C$^{\alpha}$ via ^{13}CO to ^{15}N, and ^{15}N evolves due to ^{15}N chemical shift during the ct t_1 evolution period.

The magnetization flow in the [^{15}N,^{1}H]-TROSY-HN(CA)CO experiment (Figure 1b) is

$$H_i \rightarrow \underline{N_i \rightarrow C^{\alpha}_{i,i-1}} \rightarrow CO_{i,i-1}(t_2) \rightarrow \underline{C^{\alpha}_{i,i-1} \rightarrow N_i(t_1)} \rightarrow \underline{H_i(t_3)} \quad (2)$$

where the indices $C^{\alpha}_{i,i-1}$ and $CO_{i,i-1}$ indicate that the coherence is transferred to both the sequentially and the intraresidually adjoining ^{13}C$^{\alpha}$ and ^{13}CO groups, respectively. The magnetization is transferred from ^{1}H through ^{15}N and ^{13}C$^{\alpha}$ to ^{13}CO (time point *e*). During t_2, between time points *f* and *g*, ^{13}CO evolves due to the ^{13}CO chemical shift only, since ^{13}C$^{\alpha}$ and ^{15}N are decoupled. The magnetization is transferred back from ^{13}CO via ^{13}C$^{\alpha}$ to ^{15}N between time points *h* and *i*, and ^{15}N evolves during t_1.

In [^{15}N,^{1}H]-TROSY-HNCACB (Figure 1c), the coherence flow is

$$H_i \rightarrow \underline{N_i \rightarrow C^{\alpha}_{i,i-1}} \rightarrow C^{\alpha,\beta}_{i,i-1}(t_2) \rightarrow \underline{C^{\alpha}_{i,i-1} \rightarrow N_i(t_1)} \rightarrow \underline{H_i(t_3)} \quad (3)$$

where $C^{\alpha/\beta}$ represents magnetization that is distributed to ^{13}C$^{\alpha}$ and ^{13}C$^{\beta}$, and the indices $C^{\alpha}_{i,i-1}$ and $C^{\alpha,\beta}_{i,i-1}$ again indicate that coherence transfer occurs both intraresidually and sequentially. After the coherence transfer from ^{1}H via ^{15}N to ^{13}C$^{\alpha}$, the magnetization at time point *d* is relayed to the attached ^{13}C$^{\beta}$ by the COSY-type transfer between *d* and *e*,[20] and ^{13}C$^{\alpha}$ and ^{13}C$^{\beta}$ thus evolve simultaneously during t_2. Between *h* and *i* the magnetization on ^{13}C$^{\alpha/\beta}$ is collected back on ^{13}C$^{\alpha}$ and transferred to ^{15}N.

In [^{15}N,^{1}H]-TROSY-HN(CO)CACB (Figure 1d) we have the coherence flow

$$H_i \rightarrow \underline{N_i \rightarrow CO_{i-1}} \rightarrow C^{\alpha}_{i-1} \rightarrow C^{\alpha/\beta}_{i-1}(t_2) \rightarrow C^{\alpha}_{i-1} \rightarrow \underline{CO_{i-1} \rightarrow N_i(t_1)} \rightarrow \underline{H_i(t_3)} \quad (4)$$

The magnetization transfer is similar as for [^{15}N,^{1}H]-TROSY-HN(CO)-CA (Figure 1a), except that the coherence on ^{13}C$^{\alpha}$ at time point *e* is partly transferred to ^{13}C$^{\beta}$ between *e* and *f*, as in (3). Thus, [^{15}N,^{1}H]-TROSY-HN(CO)CACB differs from [^{15}N,^{1}H]-TROSY-HN(CO)CA only by the simultaneous evolution of both ^{13}C$^{\alpha}$ and ^{13}C$^{\beta}$ during t_2[20].

The maximal ^{15}N evolution time, t_{1max}, in all the experiments of Figure 1 is limited by the ct period *T*, which was no limitation in the spectra shown in this paper. If desired, t_{1max} could be doubled by using the approach introduced in the [^{15}N,^{1}H]-TROSY-HNCA,[10] where both the ^{15}N−^{13}C out- and ^{13}C−^{15}N back-transfer times are used for the ^{15}N evolution. This technique would be applicable to all the triple-resonance experiments in this paper.

The recent implementation of TROSY into the triple resonance experiment HNCA for use with protonated proteins resulted in a 1.5-fold sensitivity enhancement when compared to conventional HNCA.[10] Although the pulse sequences of Figure 1 have been designed for use with ^{2}H/^{13}C/^{15}N-labeled proteins, they can in principle readily be adapted for protonated proteins by replacing deuterium decoupling with selective decoupling of the α-protons in Figure 1, parts a and b, and the α- and β-protons in Figure 1, parts c and d, respectively.

Results and Discussion

For all four pulse sequences in Figure 1 and their conventional counterparts without TROSY, experiments were performed with the 23 kDa ^{2}H/^{13}C/^{15}N-labeled gyrase-23B at 750 MHz. Figure 2a shows [ω_2(^{13}C),ω_3(^{1}H)] strips from a 3D [^{15}N,^{1}H]-TROSY-HN(CA)CO spectrum and Figure 2b the corresponding strips from a conventional HN(CA)CO[21] experiment recorded with

(16) DeMarco, A.; Wüthrich, K. *J. Magn. Reson.* **1976**, *24*, 201−204.
(17) Güntert, P.; Dötsch, V.; Wider, G.; Wüthrich, K. *J. Biomol. NMR* **1992**, *2*, 619−629.
(18) Bartels, C.; Xia, T.; Billeter, M.; Güntert, P.; Wüthrich, K. *J. Biomol. NMR* **1995**, *5*, 1−10.
(19) Grzesiek, S.; Bax, A. *J. Am. Chem. Soc.* **1993**, *115*, 12593−12594.
(20) Grzesiek, S.; Bax, A. *J. Am. Chem. Soc.* **1992**, *114*, 6291−6292. Grzesiek, S.; Bax, A. *J. Magn. Reson.* **1992**, *99*, 201−207. Wittekind, M.; Mueller, L. *J. Magn. Reson. B* **1993**, *101*, 201−205.
(21) Matsuo, H.; Li, H.; Wagner, G. *J. Magn. Reson. B* **1996**, *110*, 112−115.

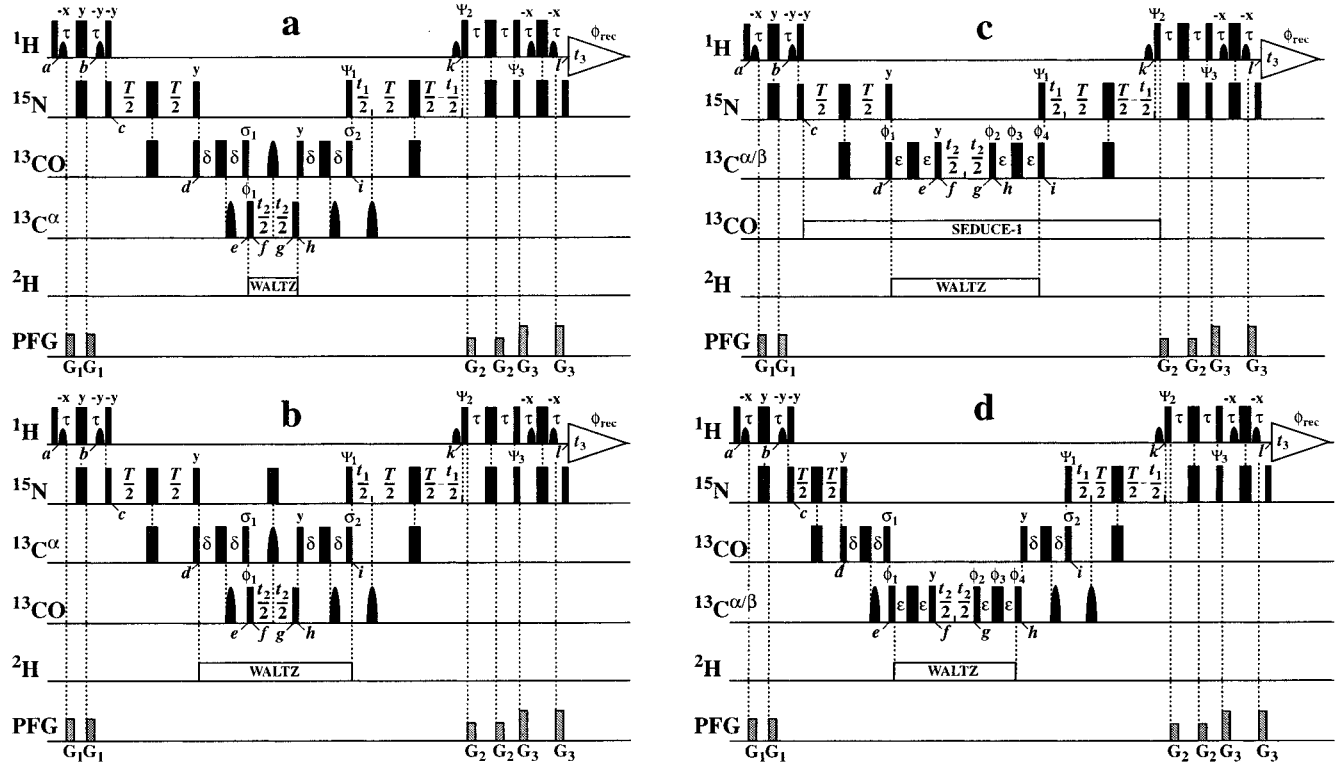

Figure 1. Experimental schemes for [^{15}N,^{1}H]-TROSY triple-resonance NMR experiments for use with deuterated proteins (for the modifications needed for work with protonated proteins, see ref 10): (a) [^{15}N,^{1}H]-TROSY-HN(CO)CA, (b) [^{15}N,^{1}H]-TROSY-HN(CA)CO, (c) [^{15}N,^{1}H]-TROSY-HNCACB, (d) [^{15}N,^{1}H]-TROSY-HN(CO)CACB. The radio frequency (rf) pulses on ^{1}H, ^{15}N, ^{13}CO, ^{13}C$^{\alpha}$, ^{13}C$^{\alpha/\beta}$, and ^{2}H are applied at 4.8, 119, 174, 55, 46, and 3.8 ppm, respectively. Narrow and wide black bars indicate nonselective 90° and 180° pulses, respectively. On the line marked ^{1}H, sine bell shapes indicate selective 90° pulses with a duration of 1 ms, a rectangular shape, and a strength of 250 Hz applied on-resonance with the water line. Sine bell shapes on the lines marked ^{13}CO, ^{13}C$^{\alpha}$, and ^{13}C$^{\alpha/\beta}$, respectively, indicate selective off-resonance 180° pulses at the corresponding frequencies with a duration of 98 μs and a Gaussian shape. The line marked PFG indicates durations and amplitudes of pulsed magnetic field gradients applied along the *z*-axis: G_1, 800 μs, 15 G/cm; G_2, 800 μs, 9 G/cm; G_3, 800 μs, 22 G/cm. The delays are $\tau = 2.7$ ms, $\delta = 4.0$ ms, $\epsilon = 3.55$ ms, and $T = 21.8$ ms. In all four experiments the same phase cycle is applied, with the phases $\Psi_1 = \{y, -y, -x, x\}$, $\Psi_2 = \{-y\}$, $\Psi_3 = \{-y\}$, $\phi_1 = \{4x, 4(-x)\}$, and $\phi_{rec} = \{y, -y, -x, x, -y, y, x, -x\}$. In parts c and d the additional rf pulses ϕ_2, ϕ_3, and ϕ_4 are applied with phases *y*, *x*, and *x*, respectively. All other rf pulses are applied with phase *x*. In parts a, b, and d off-resonance effects on ^{13}CO and ^{13}C$^{\alpha}$ produced by the shaped pulses on ^{13}C$^{\alpha}$, ^{13}C$^{\alpha/\beta}$, and ^{13}CO are corrected by the addition of appropriate phase differences to the phases $\sigma_1 = y$ and $\sigma_2 = x$. In the ^{15}N(t_1) dimension a phase-sensitive spectrum is obtained by recording a second FID for each increment of t_1, with $\Psi_1 = \{y, -y, x, -x\}$; $\Psi_2 = \{y\}$; $\Psi_3 = \{y\}$, and the data are processed as described by Kay et al.[24] Quadrature detection in the ^{13}C(t_2) dimension is achieved by the States-TPPI method[25] applied to the phase ϕ_1 in parts a and b and to the phases ϕ_2, ϕ_3, and ϕ_4 in parts c and d. The water magnetization stays aligned along the +*z*-axis throughout the experiments by the use of water flip-back pulses[19] at times *a*, *b*, and *k*. Residual transverse water magnetization is suppressed by a WATERGATE sequence[26] immediately before data acquisition. For ^{2}H-decoupling, WALTZ-16[27] was used with a field strength of 2.5 kHz. Special features of the individual experimental schemes are the following: In parts a, b, and d, 908 and 1808 pulses on ^{13}CO, ^{13}C$^{\alpha}$, and ^{13}C$^{\alpha/\beta}$ are applied with field strenghts of 6.33 and 13.89 kHz, respectively, so that their application produces minimal excitation on the ^{13}C$^{\alpha}$ and ^{13}CO frequencies, respectively. In part c, ^{13}CO decoupling is performed by using off-resonance SEDUCE-1[28] with a field strength of 0.83 kHz, which allows the application of strong rf pulses on the ^{13}C$^{\alpha/\beta}$ channel with a field strength of 21 kHz to excite the complete chemical shift range of the α- and β-carbons from approximately 10−80 ppm. In part a the ^{13}C carrier is switched from 174 to 55 ppm at time point *e* and returned to 174 ppm at point *h*; in part b, the ^{13}C carrier is switched from 55 to 174 ppm at point *e* and returned to 55 ppm at point *h*, and in part d the ^{13}C carrier is switched from 174 to 46 ppm at time point *e* and returned to 174 ppm at point *h*.

identical conditions. The strips were taken at the ^{15}N chemical shifts of residues 223−228, and the dotted line in Figure 2a indicates the "sequential walk" from the intraresidual peak at $\omega_1(^{15}N_{i-1})/\omega_2(^{13}CO_{i-1})/\omega_3(^{1}H^{N}_{i-1})$, through the sequential peak at $\omega_1(^{15}N_i)/\omega_2(^{13}CO_{i-1})/\omega_3(^{1}H^{N}_{i-1})$, to the next intraresidual peak at $\omega_1(^{15}N_i)/\omega_2(^{13}CO_i)/\omega_3(^{1}H^{N}_{i})$. With the use of [^{15}N,^{1}H]-TROSY-HN(CA)CO, all sequential $^{1}H^{N-13}CO$ connectivities in the gyrase-23B could be identified (Figure 2a), whereas with conventional HN(CA)CO no reliable sequential assignment was possible (Figure 2b).

Figure 3a presents [$\omega_2(^{13}C)$,$\omega_3(^{1}H)$] strips from a 3D [^{15}N,^{1}H]-TROSY-HNCACB spectrum, taken at the ^{15}N chemical shifts of residues 69−74. The corresponding strips from a conventional 3D HNCACB[6] spectrum are shown in Figure 3b. All sequential $^{1}H^{N-13}C^{\alpha}$ and $^{1}H^{N-13}C^{\beta}$ connectivities could be identified in [^{15}N,^{1}H]-TROSY-HNCACB, as indicated by the broken lines (Figure 3a), whereas only a small fraction of the connectivities could be identified in the corresponding conventional HNCACB spectrum (Figure 3b).

For a more quantitative assessment of the gain in signal-to-noise from the use of TROSY in triple-resonance experiments, Figure 4 presents cross sections along the $\omega_3(^{1}H)$ dimension through peaks from the following spectra: (a) 3D [^{15}N,^{1}H]-TROSY-HN(CO)CA (Figure 1a); (a′) HN(CO)CA;[6] (b) [^{15}N,^{1}H]-TROSY-HN(CA)CO (Figure 1b); (b) HN(CA)CO;[21] (c) [^{15}N,^{1}H]-TROSY-HNCACB (Figure 1c); (c′) HNCACB;[6] (d) [^{15}N,^{1}H]-TROSY-HN(CO)CACB (Figure 1d); (d′) HN(CO)CACB.[6] In general, the sensitivity in the spectra obtained with the TROSY-type experiments of Figure 1 is significantly enhanced (Figure 4a−d) when compared with the results obtained with the

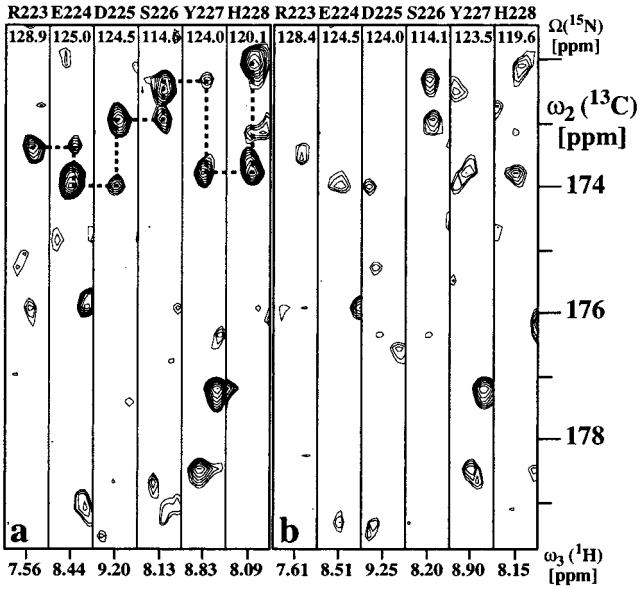

Figure 2. Comparison of corresponding [$\omega_2(^{13}C^{\alpha}),\omega_3(^1H)$] strips from two 3D experiments recorded with a 1 mM solution of uniformly $^2H/^{13}C/^{15}N$-labeled gyrase 23B: (a) [$^{15}N,^1H$]-TROSY-HN(CA)CO (Figure 1b); (b) conventional HN(CA)CO.[21] The strips were taken at the ^{15}N chemical shifts of residues 223−228 and are centered about the corresponding $^1H^N$ chemical shifts. At the top the sequence-specific assignments are indicated by the one-letter amino acid symbol and the number of the residue in the amino acid sequence. In part a those sequential connectivities that could be reliably identified are indicated by dashed lines. Since no $^1H^N$ and ^{15}N broad band decoupling is used in TROSY, the amide $^1H^N$ and ^{15}N resonances in part a are shifted by about 45 Hz relative to the corresponding resonances in part b. In the conventional HN(CA)CO experiment, DIPSI-2[29] decoupling (field strength 3.13 kHz) was used for ^1H decoupling, WALTZ-16 (2.5 kHz) was used for ^2H decoupling during t_2, and WALTZ-16 (1.6 kHz) was applied for ^{15}N decoupling during acquisition.

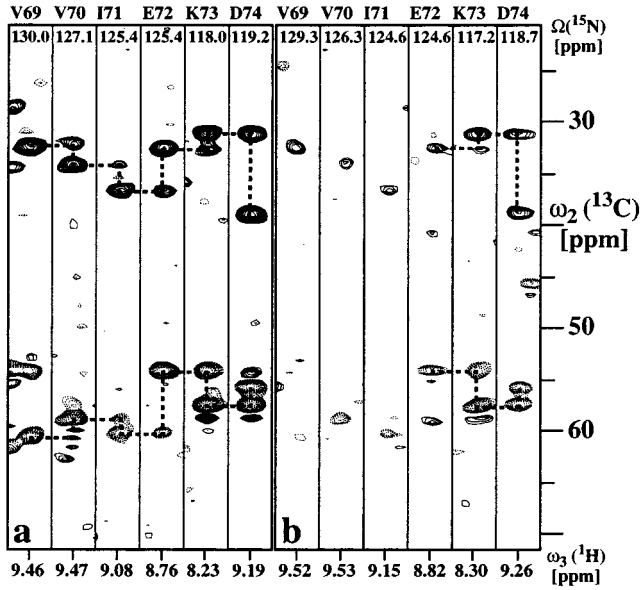

Figure 3. Comparison of corresponding [$\omega_2(^{13}C^{\alpha}),\omega_3(^1H)$] strips from two 3D experiments recorded with a 1 mM solution of uniformly $^2H/^{13}C/^{15}N$-labeled gyrase 23B: (a) [$^{15}N,^1H$]-TROSY-HNCACB (Figure 1c); (b) conventional HNCACB.[6] Same presentation as in Figure 2. The same decoupling routines were used in the conventional HNCACB experiment as described in Figure 2 for HN(CA)CO.

corresponding conventional NMR experiments (Figure 4a′−d′). For the HN(CA)CO (Figure 4b−b′) and the HN(CO)CACB

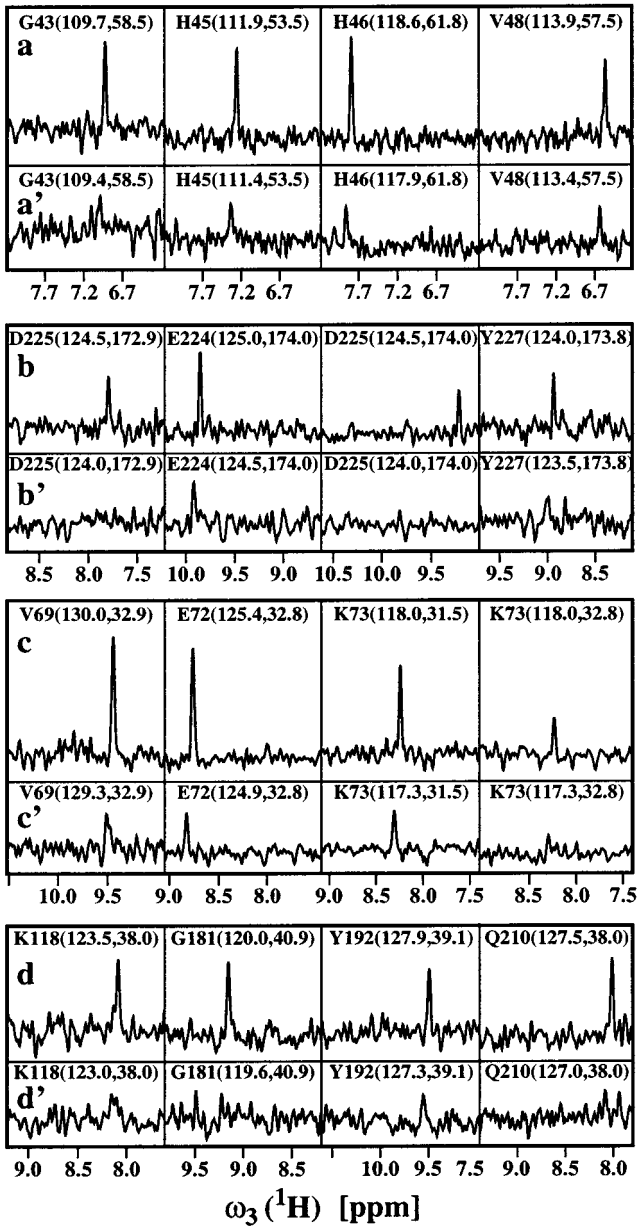

Figure 4. Cross sections along the $\omega_3(^1H)$ dimension through individual peaks in the following 3D spectra: (a) [$^{15}N,^1H$]-TROSY-HN(CO)CA (Figure 1a); (a′) conventional HN(CO)CA.[6] (b) [$^{15}N,^1H$]-TROSY-HN(CA)CO (Figure 1b); (b′) conventional HN(CA)CO.[21] (c) [$^{15}N,^1H$]-TROSY-HNCACB (Figure 1c); (c′) conventional HNCACB.[6] (d) [$^{15}N,^1H$]-TROSY-HN(CO)CACB (Figure 1d); (d′) conventional HN(CO)CACB.[6] The experimental conditions used are described in the captions to Figures 1 and 2. In each panel the observed peak is identified by the one-letter amino acid symbol and the residue number in the amino acid sequence, and the $\omega_1(^{15}N)$ and $\omega_2(^{13}C)$ chemical shifts are indicated in parentheses.

experiments (Figure 4d−d′), workable signal intensities were obtained only with TROSY.

The intensities of all peaks in the 3D spectra of gyrase-23B were determined and compared for each pair of experiments recorded with and without [$^{15}N,^1H$]-TROSY. Figure 5 shows these data for [$^{15}N,^1H$]-TROSY-HN(CO)CA and conventional HN(CO)CA.[6] For almost all sequential $\omega_1(^{15}N_i)/\omega_2(^{13}C^{\alpha}_{i-1})/\omega_3(^1H^N_i)$ correlation peaks the [$^{15}N,^1H$]-TROSY-HN(CO)CA experiment yields significant improvements in sensitivity compared to the conventional HN(CO)CA experiment. In line with theoretical predictions[10,11] the highest sensitivity gains were

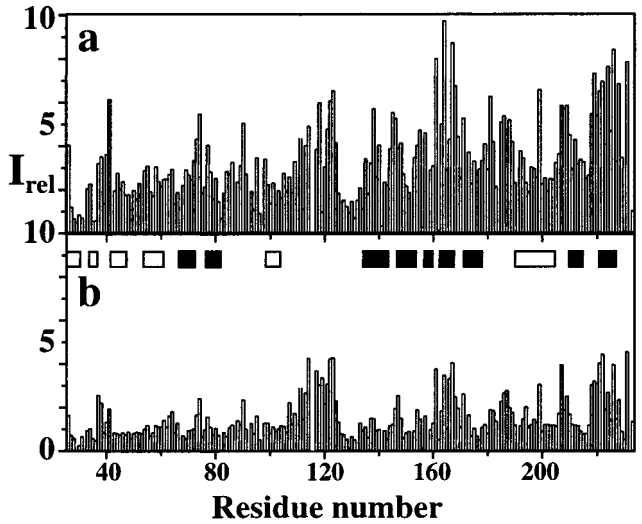

Figure 5. Plots of relative signal intensities, I_{rel}, versus the amino acid sequence of uniformly $^2H/^{13}C/^{15}N$-labeled gyrase 23B (1 mM, 95% H_2O/5% D_2O at pH 6.5 and $T = 20$ °C). (a) Sequential correlation peaks ($\omega_2(^{13}C^{\alpha}_{i-1})/\omega_3(^1H_i)$) in [$^{15}N$,$^1H$]-TROSY-HN(CO)CA (Figure 1a). (b) Same as part a measured with conventional HN(CO)CA.[6] Both spectra were recorded with the same experimental conditions and processed identically, as described in the text. The α-helical and β-sheet regions in the X-ray structure of gyrase 23B[14] are identified in panel b as open and filled bars, respectively.

Table 1 Sensitivity Gains Obtained with $^2H/^{13}C/^{15}N$-Labeled Gyrase 23B When Using [^{15}N,^1H]-TROSY in Triple Resonance Experiments

	enhancement[a]		
experiment	overall	β-sheets	α-helices
[^{15}N,^1H]-TROSY-HN(CO)CA[b]	2.3	3.1	2.6
[^{15}N,^1H]-TROSY-HN(CA)CO[c]	3.2	3.9	3.4
[^{15}N,^1H]-TROSY-HNCACB[d]	2.8	3.4	2.9
[^{15}N,^1H]-TROSY-HN(CO)CACB[e]	3.1	3.4	3.3

[a] Signal-to-noise ratio in the experiment with TROSY divided by the signal-to-noise ratio in the conventional experiment. Pairs of corresponding peaks were compared and the average taken either for the entire protein, the α-helices, or the β-sheets. [b] Average calculated from all detected peaks at $\omega_1(^{15}N_i)/\omega_2(^{13}C^{\alpha}_{i-1})/\omega_3(^1H^N_i)$; missing peaks in conventional HN(CO)CA, which were present in [^{15}N,^1H]-TROSY-HN(CO)CA, were assigned to the noise-value. [c] Average calculated from all detected peaks at $\omega_1(^{15}N_i)/\omega_2(^{13}CO_i)/\omega_3(^1H^N_i)$ and $\omega_1(^{15}N_i)/\omega_2(^{13}CO_{i-1})/\omega_3(^1H^N_i)$; missing peaks in conventional HN(CA)CO, which were present in [^{15}N,^1H]-TROSY-HN(CA)CO, were assigned to the noise-value. [d] Average calculated from all detected peaks at $\omega_1(^{15}N_i)/\omega_2(^{13}C^{\alpha}_i)/\omega_3(^1H^N_i)$, $\omega_1(^{15}N_i)/\omega_2(^{13}C^{\beta}_i)/\omega_3(^1H^N_i)$, $\omega_1(^{15}N_i)/\omega_2(^{13}C^{\alpha}_{i-1})/\omega_3(^1H^N_i)$, and $\omega_1(^{15}N_i)/\omega_2(^{13}C^{\beta}_{i-1})/\omega_3(^1H^N_i)$; missing peaks in conventional HNCACB, which were present in [^{15}N,^1H-TROSY-HNCACB, were assigned to the noise-value. [e] Average calculated from all detected peaks at $\omega_1(^{15}N_i)/\omega_2(^{13}C^{\alpha}_{i-1})/\omega_3(^1H^N_i)$ and $\omega_1(^{15}N_i)/\omega_2(^{13}C^{\beta}_{i-1})/\omega_3(^1H^N_i)$; missing peaks in conventional HN(CO)CACB, which were present in [^{15}N,^1H]-TROSY-HN(CO)CACB, were assigned to the noise-value.

obtained for the regular secondary structure elements in the protein core, whereas for the flexible parts, for example, around residue 120, TROSY yields similar signal intensity as the conventional experiments.

Table 1 lists the enhancement factors obtained with the experiments of Figure 1 when compared to their conventional counterparts. The average enhancements over the entire amino acid sequence of gyrase-23B are 2.3-fold for [^{15}N,^1H]-TROSY-HN(CO)CA, 3.2-fold for [^{15}N,^1H]-TROSY-HN(CA)CO, 2.8-fold for [^{15}N,^1H]-TROSY-HNCACB, and 3.1-fold for [^{15}N,^1H]-TROSY-HN(CO)CACB. The sensitivity gains for α-helical and β-sheet regions are slightly higher than the average, in the extent of 6−13% and 10−35%, respectively.

Together with the previously described [^{15}N,^1H]-TROSY-HNCA and [^{15}N,^1H]-TROSY-HNCO schemes,[10] the experiments of Figure 1 represent a complete set of measurements for obtaining sequential assignment in proteins. [^{15}N,^1H]-TROSY-HN(CO)CA (Figure 1a), which detects only the sequential correlation peak with $^{13}C^{\alpha}(i-1)$ at the $^1H^N(i)/^{15}N(i)$ position of residue i, complements the [^{15}N,^1H]-TROSY-HNCA experiment,[10] and allows a distinguishion to be made between the $^{13}C^{\alpha}(i)$ and $^{13}C^{\alpha}(i-1)$ peaks in [^{15}N,^1H]-TROSY-HNCA.[4,10] Similarly, [^{15}N,^1H]-TROSY-HN(CA)CO and [^{15}N,^1H]-TROSY-HNCO[10] can be combined.[22,23] In principle, the HN(CA)CO/HNCO pair of experiments is to be preferred over the HNCA/HN(CO)CA pair, since the spectral resolution is higher for ^{13}CO than for $^{13}C^{\alpha}$.[22,23] The improved sensitivity of [^{15}N,^1H]-TROSY-HN(CA)CO may actually make the use of this combination a valid alternative.

In conclusion, the implementation of TROSY in triple-resonance experiments for the sequential assignment of $^2H/^{13}C/^{15}N$-labeled proteins shows significant gains in sensitivity compared to the corresponding conventional experiments. The enhancements are most pronounced for regular secondary structure elements in the protein (Table 1). The gain in sensitivity is of particular interest for [^{15}N,^1H]-TROSY-HN(CA)CO (Figure 1b) and [^{15}N,^1H]-TROSY-HNCACB (Figure 1c), since these two experiments reveal both sequential and intraresidual correlation peaks and thus allow the determination of sequential connectivities in a single experiment. In practical applications of these two triple-resonance experiments, the TROSY-type pulse schemes enabled a much more complete identification of sequential correlation peaks than the conventional spectra.

Although all the experimental results presented here were obtained with a $^2H/^{13}C/^{15}N$-labeled protein, corresponding pulse schemes for use with protonated proteins can readily be designed.[10] A theoretical analysis of the transverse relaxation of ^{15}N in triple-resonance experiments showed that ^{15}N relaxation is only little affected by the additional protons in a nondeuterated protein,[10] and hence the TROSY principle yields significant improvement of sensitivity also in protonated proteins.

Acknowledgment. Financial support was obtained from the Schweizerischer Nationalfonds (project 31.49047.96). We thank Bernard Gsell for his help in preparing the gyrase 23B.

JA9834226

(22) Grzesiek, S.; Bax, A. *J. Magn. Reson.* **1992**, *96*, 432−440.
(23) Clubb, R. T.; Thanabal, V.; Wagner, G. *J. Magn. Reson.* **1992**, *97*, 213−217. Engelke, J.; Rüterjans, H. *J. Magn. Reson. B* **1995**, *109*, 318−322.
(24) Kay, L. E.; Keifer, P.; Saarinen, T. *J. Am. Chem. Soc.* **1992**, *114*, 10663−10664.
(25) Marion, D.; Ikura, M.; Tschudin, R.; Bax, A. *J. Magn. Reson.* **1989**, *85*, 393−399.
(26) Piotto, M.; Saudek, V.; Sklenar, V. J. *J. Biomol. NMR* **1992**, *2*, 661−665.
(27) Shaka, A. J.; Keeler, J.; Frenkiel, T.; Freeman, R. *J. Magn. Reson.* **1983**, *52*, 335−338.
(28) McCoy, M. A.; Mueller, L. *J. Am. Chem. Soc.* **1992**, *114*, 2108−2112.
(29) Cavanagh, J.; Rance, M. *J. Magn. Reson.* **1992**, *96*, 670−678.